(Tetramethylthiophene)ruthenium Dichloride Dimer: A Versatile Synthetic Intermediate in Thiophene Coordination Chemistry

John R. Lockemeyer,[1] Thomas B. Rauchfuss,*[,1] Arnold L. Rheingold,[2] and Scott R. Wilson[1]

Contribution from the School of Chemical Sciences, University of Illinois at Urbana—Champaign, 505 South Mathews Avenue, Urbana, Illinois 61801, and the Department of Chemistry, University of Delaware, Newark, Delaware 19711. *Received May 10, 1989*

Abstract: The thermal reaction of $[(\text{cymene})RuCl_2]_2$ and tetramethylthiophene (TMT) gives $[(TMT)RuCl_2]_2$ (**1**). Treatment of **1** with silver salts in the presence of various ligands gives salts of $[(TMT)RuL_3]^{2+}$ where $L_3 = (H_2O)_3$, $(CH_3CN)_3$, and TMT. A crystallographic study demonstrated that $[(TMT)_2Ru](BF_4)_2 \cdot 2CH_3NO_2$ adopts a sandwich structure with sulfur atoms sited cis on the pseudooctahedron. Cyclic voltammetry studies show that $[(TMT)_2Ru]^{2+}$ undergoes two reversible one-electron reductions. Solutions of **1** and phosphine and amine donors react to give well-behaved monometallic derivatives of the type $(TMT)RuCl_2L$ where L is PR_3 and $NH_2C_6H_4Me$. For bulky L = PPh_3 and $P(C_6H_4Me)_3$, variable-temperature NMR studies demonstrate hindered rotation about the Ru-P and Ru···TMT axes. Treatment of **1** with $(Me_3Si)_2S$ gives the cluster $[(TMT)RuCl]_3S^+$ whose PF_6^- salt was examined by X-ray crystallography. The cluster is comprised of three conjoined pseudooctahedral Ru centers bridged by one μ_3-S and three μ-Cl atoms.

There is currently much interest in the interaction of metals and thiophenes.[3,4] Studies have focused on the metals themselves, partially sulfided single crystals, and a variety of metal complexes in solution. The goal of this research is the elucidation of the ways by which metals can facilitate the desulfurization of these heterocycles.[5] Since thiophenes are the major sulfur-containing contaminants in fossil fuels, this is an area where organometallic chemistry impacts on some important environmental and energy issues.

Thiophenes have been shown to bind to metals via four bonding modes.[6] The η^1-S-bonded mode remains rare,[7-9] but we have argued[8] that this type of interaction precedes the more prevalent η^5 coordination mode. With one exception, all known η^5-thiophene complexes are based on d^6 pseudooctahedral metal centers with the stoichiometry $(SC_4R_4)ML_3$ where $L_3 = (CO)_3$,[10] C_5R_5,[4,11] C_6R_6,[11] and SC_4R_4.[12] The very labile $[(SC_4R_4)Rh(L)_2]^+$ (L = PR_3,[13] olefin[11]) are the exception. Very recently η^2- and η^4-thiophene ligands have been identified.[14] In none of these cases can the ancillary ligands be easily substituted.

In this report, we describe what we believe to be the first thiophene complexes with replaceable coligands. This feature permits the preparation of a broad range of derivatives including the first thiophene–metal–sulfido cluster, a model for thiophene chemisorbed on a metal sulfide catalyst.

Results

$[(TMT)RuCl_2]_2$. (Tetramethylthiophene)ruthenium dichloride dimer (**1**) was prepared by the thermal arene exchange of 2,3,4,5-tetramethylthiophene (TMT) with $[(p\text{-cymene})RuCl_2]_2$ (p-cymene is 4-isopropyltoluene, eq 1). The synthesis conditions call for an excess of TMT and reaction temperatures greater than the boiling point of p-cymene (bp 176–178 °C). Although the details of the process were not investigated, the synthesis is thought to be driven by the volatilization of p-cymene.

$[(p\text{-cymene})RuCl_2]_2 + 2TMT \rightarrow$

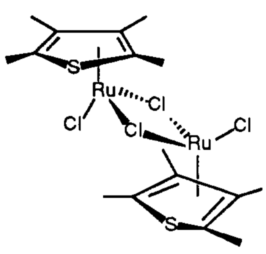

$+ 2(p\text{-cymene})$ (1)

1

Once formed, **1** is air stable in solution as well as in the solid state. The solution properties of **1** resemble those of the parent cymene dimer. It is stable in noncoordinating organic solvents such as CH_2Cl_2 or $CHCl_3$ in which it most likely exists as the dimer. Its ^1H NMR spectrum consists of two singlets. The ^{13}C NMR chemical shifts for the ring carbons appear 40 ppm upfield of free TMT.

Solutions of **1** in D_2O give an NMR spectrum indicative of two species, the ~10:1 ratio of which remains unchanged over a period of weeks. The minor species is $[(TMT)Ru(D_2O)_3]^{2+}$,[15] confirmed by treatment of such aqueous solutions with excess $AgBF_4$. We also generated solutions of $[(TMT)Ru(CH_3CN)_3]^{2+}$ in acetonitrile

---

[1] University of Illinois.

[2] University of Delaware.

[3] Leading references can be found in: Ogilvy, A. E.; Draganjac, M.; Rauchfuss, T. B. *Organometallics* **1988**, *7*, 1171.

[4] Angelici, R. J. *Acc. Chem. Res.* **1988**, *21*, 389.

[5] (a) Zonnevylle, M. C.; Hoffmann, R.; Harris, S. *Surf. Sci.* **1988**, *199*, 320. (b) Gates, B. C.; Katzer, J. R.; Schuit, G. C. A. *Chemistry of Catalytic Processes*; McGraw Hill: New York, 1974.

[6] The η^1- and η^5-bonding modes are also observed on surfaces; see: Lang, J. F.; Masel, R. I. *Surf. Sci.* **1987**, *44*, 183.

[7] Bucknor, S. M.; Draganjac, M. E.; Rauchfuss, T. B.; Ruffing, C. J.; Fultz, W. C.; Rheingold, A. L. *J. Am. Chem. Soc.* **1984**, *106*, 5379.

[8] Draganjac, M.; Ruffing, C. J.; Rauchfuss, T. B. *Organometallics* **1985**, *4*, 1909.

[9] Goodrich, J. D.; Nickias, P. N.; Selegue, J. P. *Inorg. Chem.* **1987**, *26*, 3424.

[10] Fischer, E. O.; Öfele, K. *Chem. Ber.* **1958**, *91*, 2395.

[11] Russell, M. J. H.; White, C.; Yates, A.; Maitlis, P. M. *J. Chem. Soc., Dalton Trans.* **1978**, 857. Huckett, S. C.; Miller, L. L.; Jacobson, R. A.; Angelici, R. J. *Organometallics* **1988**, *7*, 686.

[12] Braitsch, D. M.; Kumarappan, R. *J. Organometal. Chem.* **1975**, *84*, C57. Guerchais, V.; Astruc, D. *J. Organomet. Chem.* **1986**, *316*, 335.

[13] Sanchez-Delgado, R. A.; Marquez-Silva, R. L.; Puga, J.; Tiripicchio, A.; Tiripicchio-Camellini, M. *J. Organometal. Chem.* **1986**, *316*, C35.

[14] η^4-Thiophene complexes: see: Reference 21. Angelici, R. J.; Chen, J. *Abstracts of Papers*, 198th National Meeting of the Americal Chemical Society, Miami Beach, FL; American Chemical Society: Washington, DC, 1989; INOR 351. η^2-Thiphene: Cordone, R.; Harman, W. D.; Taube, H. *J. Am. Chem. Soc.* **1989**, *111*, 5969.

[15] Studies on $[(\text{arene})M(H_2O)_3]^{2+}$: Hung, Y.; Kung, W.-J.; Taube, H. *Inorg. Chem.* **1981**, *20*, 457. Stebler-Röthlisberger, M.; Hummel, W.; Pittet, P.-A.; Bürgi, H.-B.; Ludi, A.; Merbach, A. E. *Inorg. Chem.* **1988**, *27*, 1358. Gould, R. A.; Jones, L. L.; Robertson, D. R.; Stephenson, T. A. *J. Chem. Soc., Chem. Commun.* **1977**, 222.

0002-7863/89/1511-8828$01.50/0

Table I. Selected Bond Distances, Angles, and Planes for $[(TMT)_2Ru](BF_4)_2 \cdot 2CH_3NO_2$

(a) Bond Distances, Å

Ru-CNT1	1.825 (7)	Ru-C12	2.239 (9)
Ru-CNT2	1.819 (7)	S1-C1	1.767 (10)
Ru-S1	2.359 (2)	S1-C4	1.777 (8)
Ru-S2	2.351 (2)	S2-C9	1.766 (8)
Ru-C1	2.222 (10)	S2-C12	1.700 (11)
Ru-C2	2.261 (9)	C1-C2	1.390 (12)
Ru-C3	2.211 (9)	C2-C3	1.427 (15)
Ru-C4	2.196 (9)	C3-C4	1.393 (12)
Ru-C9	2.187 (9)	C9-C10	1.399 (14)
Ru-C10	2.223 (8)	C10-C11	1.392 (12)
Ru-C11	2.248 (10)	C11-C12	1.471 (12)

(b) Bond Angles, deg

CNT1-Ru-CNT2	172.5 (3)	C2-C3-C4	114.7 (8)
S1-Ru-S2	121.8 (1)	C3-C4-S1	109.7 (7)
C1-S1-C4	91.6 (4)	S2-C9-C10	111.0 (6)
C9-S2-C12	92.0 (4)	C9-C10-C11	115.0 (7)
S1-C1-C2	111.2 (8)	C10-C11-C12	112.3 (9)
C1-C2-C3	112.5 (8)	C11-C12-S2	109.4 (6)

(c) Best Planes (atom, δÅ)[a]

plane 1 S1, 0.031 (2); C1, -0.036 (8); C2, 0.025 (8); C3, 0.006 (8); C4, -0.025 (8)
external: Ru, -1.824 (1); C5, -0.013 (10); C6, 0.086 (12); C7, 0.091 (12); C8, 0.067 (12)

plane 2 S2, 0.023 (2); C9, -0.025 (8); C10, 0.015 (8); C11, 0.008 (8); C12, -0.021 (9)
external: Ru, -1.818 (1); C13, 0.086 (12); C14, 0.126 (12); C15, 0.074 (13); C16, 0.052 (12)

[a] Negative values indicate that the atom lies on the Ru side of the best C_4S plane.

via an analogous metathesis route. Over a period of hours, this complex decomposes in acetonitrile solution to give colorless $[Ru(CH_3CN)_6]^{2+}$ concomitant with formation of free TMT.[16] Apparently, the donor/acceptor properties of the ancillary ligands strongly influence the lability of the TMT.

$[(TMT)_2Ru]^{2+}$. This compound was prepared by the addition of 4 equiv of AgX (X = BF_4^-, OTf^-) to a mixture of **1** and excess TMT in acetone (eq 2). While the solvated intermediate was

$$[(Me_4C_4S)RuCl_2]_2 + 2Me_4C_4S + 4Ag^+ \rightarrow 2[(Me_4C_4S)_2Ru]^{2+} + 4AgCl \quad (2)$$

not isolated, related arene complexes are known.[17] $[(TMT)_2Ru]^{2+}$ was isolated as a yellow air-stable BF_4^- salt which is fairly robust in solution. Acetone solutions of $[(TMT)_2Ru]^{2+}$ exhibited no exchange with added benzene after 4 days at 24 °C. The complex will, however, react with hot O_2-free H_2O, giving a deep red solution in a matter of hours.[18]

Cyclic voltametric studies on $[(TMT)_2Ru]^{2+}$ show two reversible one-electron reductions centered at -392 and -568 mV vs Ag/AgCl (Figure 1). Using the expression shown in eq 3,[19] we

$$K_{disp} = \exp\left\{-\frac{nF}{RT}\Delta E^0\right\} = \frac{[(TMT)_2Ru^0][(TMT)_2Ru^{2+}]}{[(TMT)_2Ru^+]^2} \quad (3)$$

calculate that the disproportionation constant, k_{disp}, for $[(TMT)_2Ru]^+$ is 0.0506. This indicates that the radical cation $[(TMT)_2Ru]^+$ disproportionates to a relatively small amount. The calculation assumes that the measured $\Delta E_{1/2}$ values are identical with the ΔE^0's, which holds if the diffusion constants are the same for the three oxidation states of $[(TMT)_2Ru]^z$.

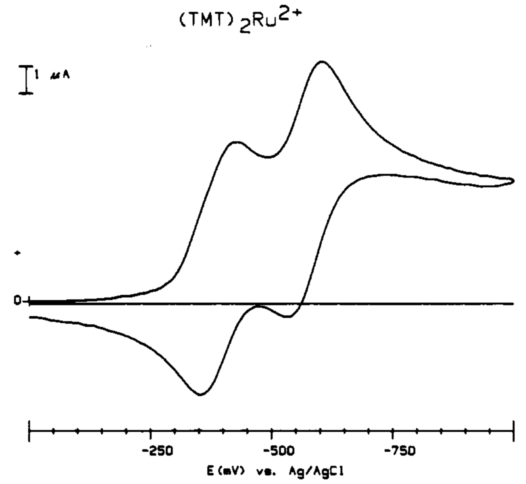

Figure 1. Cyclic voltammogram of $[(TMT)_2Ru](BF_4)_2$, 10^{-3} M in acetone. Scan rate of 100 mV/s (supporting electrolyte, 0.1 M Bu_4NPF_6).

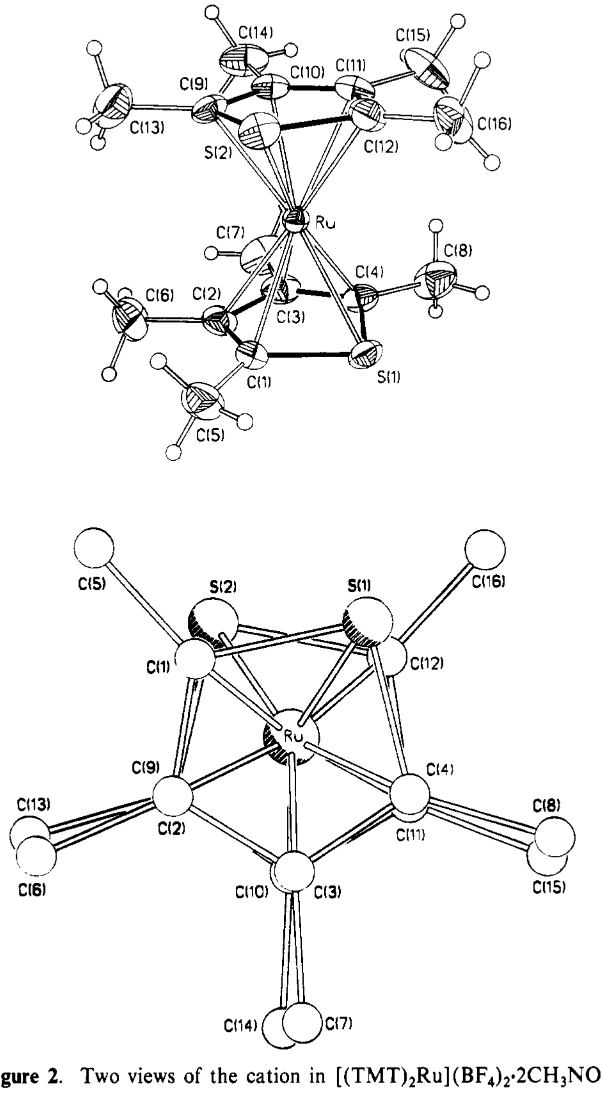

Figure 2. Two views of the cation in $[(TMT)_2Ru](BF_4)_2 \cdot 2CH_3NO_2$.

Related work has shown that $[(TMT)_2Fe]^{2+}$ and $[(TMT)FeCp]^+$ also undergo sequential one-electron reductions although in each case only the first couple was reversible.[13] The accessibility to the zero-valent species $[(TMT)_2Ru]^0$ is intriguing,[20] and work is under way to characterize the reduced species. Controlled

---

[16] $[Ru(CH_3CN)_6]^{2+}$: Schrock, R. R.; Johnson, B. F. G.; Lewis, J. *J. Chem. Soc., Dalton Trans.* **1974**, 951.

[17] A discussion of the reactivity of $[(arene)Ru(Me_2CO)_3]^{2+}$: Bennett, M. A.; Matheson, T. W.; Robertson, G. B.; Steffen, W. L.; Turney, T. W. *J. Chem. Soc., Chem. Commun.* **1979**, 32. Bennett, M. A.; Matheson, T. W. *J. Organomet. Chem.* **1979**, *175*, 87.

[18] The aqueous chemistry of $(TMT)Ru^{2+}$ will be described in a subsequent paper: Ganja, E. A.; Rauchfuss, T. B.; Wilson, S. R. Manuscript in preparation.

[19] Heinze, J. *Angew. Chem., Int. Ed. Engl.* **1984**, *23*, 831; *Angew. Chem.* **1984**, *96*, 823.

[20] Redox chemistry of metal arene complexes: Bowyer, W. J.; Merkert, J. W.; Geiger, W. E.; Rheingold, A. L. *Organometallics* **1988**, *8*, 191. Bowyer, W. J.; Geiger, W. E. *J. Am. Chem. Soc.* **1985**, *107*, 5657. Finke, R. G.; Voegeli, R. H.; Laganis, E. D.; Boekelheide, V. *Organometallics* **1983**, *2*, 347.

Scheme I

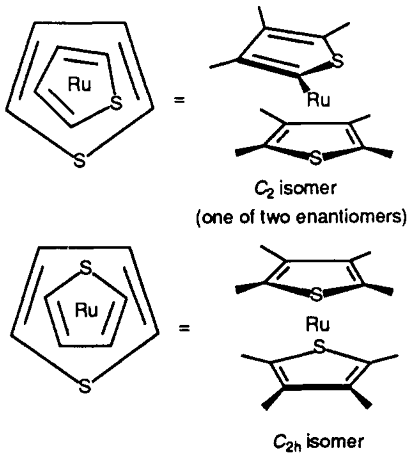

potential electrolysis of an acetone solution of [(TMT)$_2$Ru]$^{2+}$ at −1300 mV vs F_c/F_c^+ consumed 2.15 e$^-$/mol of dication. This reduction proceeds with a color change from pale yellow to maroon (at ca. 1 e$^-$/mol of dication) to deep red. Recent work on the related [Cp*Rh(TMT)]$^{2+}$ has shown that two-election reduction gives the η^4-thiophene complex.[21]

Structure of [(TMT)$_2$Ru](BF$_4$)$_2$. The (CH$_3$NO$_2$)$_2$ solvate of this salt was characterized by single-crystal X-ray diffraction (Figure 2). Selected distances, angles, and planes are listed in Table I. The wide range for the ring C–C distances in this complex initially caught our attention; however, in view of the moderate refinement, these distances are not chemically significant. With one exception, the methyl carbon atoms lay $\leq$0.126 (12) Å out of the plane of the C$_4$S core, away from the metal.

If each TMT ligand is considered to be a tridentate diolefin–thioether ligand, the complex can be viewed as possessing octahedral geometry. The ruthenium is equidistant between the two TMT ligands. The [(TMT)$_2$Ru]$^{2+}$ cations are chiral in the lattice, and the crystal contains enantiomeric pairs that are related by crystallographic mirror symmetry.

The view down the TMT (centroid)–metal–TMT (centroid) axis shows that the two sulfur atoms are mutually cis on the idealized octahedron (Figure 2). The alternative octahedral structure would involve mutually trans sulfur atoms. The C_{2h} structure necessarily positions the acceptor orbitals on the TMT ligands mutually trans. The rotational isomers for "octahedral" [(TMT)$_2$Ru]$^{2+}$ are depicted in Scheme I. The 300-MHz ^{1}H NMR spectrum of [Ru(TMT)$_2$](OTf)$_2$ in acetone is invariant at +30 to −60 °C.

(TMT)RuCl$_2$L Complexes. Complexes of this type are accessible by bridge cleavage reactions[22] on **1**. Reaction of CH$_2$Cl$_2$ solutions of **1** with 2 equiv of *tert*-phosphines gives (TMT)RuCl$_2$(PR$_3$) complexes (R = Me, Bu, Ph, *p*-tolyl) in good yields. We also prepared the complex (TMT)RuCl$_2$(*p*-toluidine).

The ^{1}H NMR spectra of (TMT)RuCl$_2$(PR$_3$) are strikingly different for R = Me, Bu vs R = Ph, *p*-tolyl. The differences can be rationalized in terms of steric interaction (or lack thereof) of the R groups with the methyl substituents on the TMT ring. For example, the ^{1}H NMR spectrum of (TMT)RuCl$_2$(PMe$_3$) in CDCl$_3$ at 24 °C displays two sharp TMT resonances as would be expected for a freely rotating TMT ligand. However, the room-temperature 300-MHz ^{1}H NMR spectrum of (TMT)RuCl$_2$(PPh$_3$) shows two very broad resonances in the TMT methyl region. These methyl resonances become two singlets when the solution temperature is raised to +60 °C. At −60 °C, we observed four methyl resonances of equal integrated intensity. Careful inspection of the spectrum in the figure shows the presence of a small impurity of free TMT. The fact that the signals for the free TMT remain distinct throughout the temperature range shows that the ligand dynamics do not involve dissociation of TMT. The complexity of the phenyl signals also increases as the temperature approaches −60 °C (Figure 3) which we ascribe to hindered rotation about the Ru–P bond. The observation of four methyl resonances is only consistent with chiral structure "A" in Scheme II wherein all four TMT methyl groups are chemically nonequivalent. This assignment is consonant with octahedral Ru(II) where the TMT is again viewed as a tridentate diolefin thioether. The chiral structure is one of two possible octahedral rotamers of (TMT)RuCl$_2$L, the stereochemical situation being completely analogous to that for [(TMT)$_2$Ru]$^{2+}$ (Scheme II).

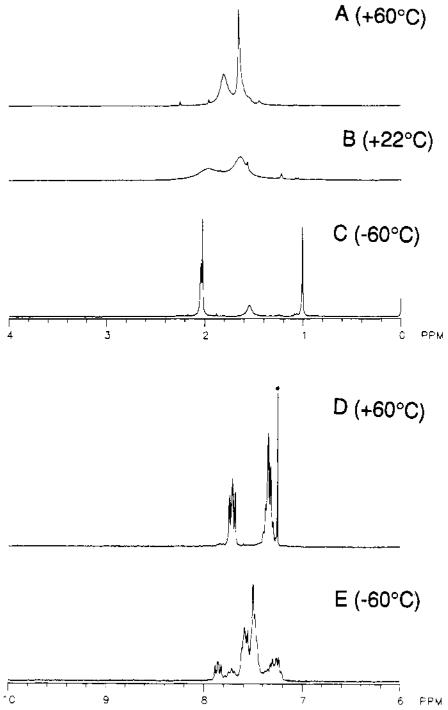

Figure 3. 300-MHz ^{1}H NMR spectra of CD$_2$Cl$_2$ solutions of (TMT)RuCl$_2$(PPh$_3$) in the methyl (A–C) and phenyl regions (D–E). Small peaks at 2.25 and 1.96 ppm in A are due to a trace of free TMT.

Scheme II

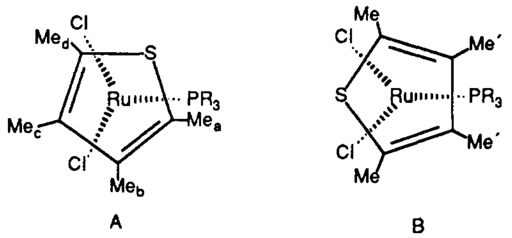

[(TMT)RuCl]$_3$S(PF$_6$). The synthesis of a Ru–S–thiophene cluster was accomplished by the reaction of [(TMT)RuCl$_2$]$_2$ with (Me$_3$Si)$_2$S followed by anion metathesis to give the PF$_6^-$ salt. The ^{1}H NMR spectrum of the product shows two singlets, indicative of equivalent TMT ligands. Elemental analysis supports the formulation of a trinuclear complex with a S:Cl ratio of 4:3. FAB mass spectrometry shows a parent ion envelope that was well simulated by the formula C$_{24}$H$_{36}$Cl$_3$Ru$_3$S$_4^+$.

The structure of this sulfido cluster was elucidated by single-crystal X-ray diffraction (Figure 4). The coordination geometry about each metal is pseudooctahedral, each ruthenium being coordinated to the μ_3-S and two μ-Cl atoms and one TMT. The Ru–ligand distances and angles are very similar for all three Ru centers; therefore, only the results for Ru1 are presented in Table II. The Ru···Ru distances are nonbonding. The Ru–μ_3-S distances range from 2.36 to 2.39 Å, which compare well with other Ru$^{\mathrm{II}}$–S single bonds[23] but are ca. 0.07 Å longer than in [(*p*-

---

[21] Ogilvy, A. E.; Skaugset, A. E.; Rauchfuss, T. B. *Organometallics*, in press.

[22] Bennett, M. A.; Smith, A. K. *J. Chem. Soc., Dalton Trans.* **1974**, 233.

[23] Amarasekera, J.; Rauchfuss, T. B.; Wilson, S. R. *Inorg. Chem.* **1987**, *26*, 3328. Kroener, R.; Heeg, M.-J.; Deutsch, E. *Inorg. Chem.* **1988**, *27*, 558.

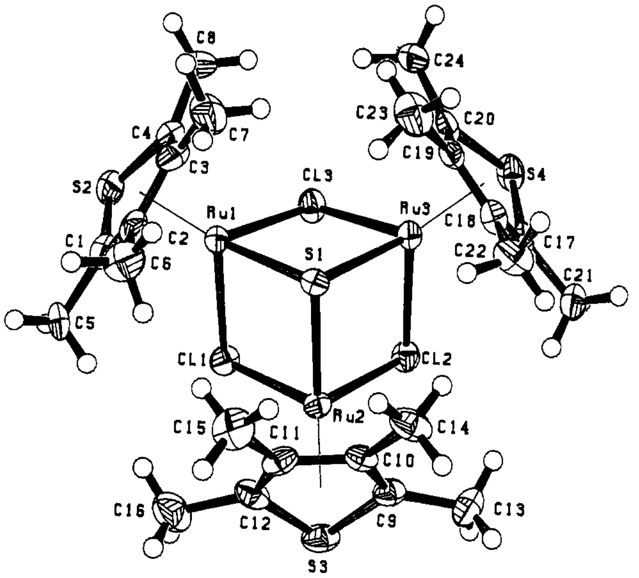

Figure 4. Structure of the cation in $[(TMT)RuCl]_3S(PF_6)$.

Table II. Selected Distances, Angles, and Planes for the Cation in $[(TMT)RuCl]_3S(PF_6)$

Selected Distances, Å			
Ru1–Cl1	2.441 (3)	Ru1–Cl3	2.446 (3)
Ru1–S1	2.387 (3)	Ru1–S2	2.414 (4)
Ru1–C1	2.11 (1)	S2–C1	1.77 (1)
Ru1–C2	2.16 (1)	C1–C2	1.39 (2)
Ru1–C3	2.16 (1)	C2–C3	1.46 (2)
Ru1–C4	2.12 (1)	S2–C4	1.81 (1)
C3–C4	1.41 (2)		
Selected Angles, deg			
Cl1–Ru1–Cl3	88.0 (1)	Cl1–Ru1–S1	82.87 (9)
Cl1–Ru1–S2	105.6 (1)	Cl1–Ru1–C1	91.6 (4)
Cl1–Ru1–C2	114.2 (3)	Cl1–Ru1–C3	153.7 (4)
Cl1–Ru1–C4	151.3 (3)	Cl3–Ru1–S1	84.31 (9)
Cl3–Ru1–S2	104.7 (1)	Cl3–Ru1–C1	148.6 (4)
Cl3–Ru1–C2	157.7 (3)	Cl3–Ru1–C3	118.2 (4)
Cl3–Ru1–C4	93.0 (3)	S1–Ru1–S2	167.6·(1)
S1–Ru1–C1	126.8 (4)	S1–Ru1–C2	97.7 (3)
S1–Ru1–C3	97.3 (4)	S1–Ru1–C4	125.8 (3)
S2–Ru1–C1	45.5 (4)	S2–Ru1–C2	70.7 (4)
S2–Ru1–C3	71.1 (4)	S2–Ru1–C4	46.4 (3)
C1–Ru1–C2	38.1 (5)	C1–Ru1–C3	67.2 (5)
C1–Ru1–C4	73.0 (5)	C2–Ru1–C3	39.5 (5)
C2–Ru1–C4	67.8 (5)	C3–Ru1–C4	38.5 (5)
Ru1–Cl1–Ru2	94.98 (10)	Ru1–S1–Ru3	96.90 (9)

(c) Best Planes (atom, δÅ)[a]

plane 1 S2, 0.076 (4); C1, −0.076 (13); C2, 0.036 (12); C3, 0.038 (13); C4, −0.075 (12)
external: Ru1, −1.747 (1); C5, −0.107 (12); C6, 0.203 (14); C7, 0.194 (15); C8, 0.003 (14)
plane 2 S3, 0.0867 (3); C9, −0.0751 (11); C10, 0.02056 (10); C11, 0.0570 (0.011); C12, 0.0942 (0.016)
external: Ru2, −1.7715 (1); C13, 0.0009 (13); C14, 0.1707 (12); C15, 0.2126 (13); C16, −0.0111 (14)
plane 3 S4, 0.0878 (3); C17, −0.0890 (12); C18, 0.0449 (12); C19, 0.0414 (11); C5, −0.0851 (12)
external: Ru3, −1.7634 (1); C21, −0.0670 (13); C22, 0.2930 (13); C23, 0.2155 (14); C24, −0.0442 (13)

[a] Negative values indicate that the atom lies on the Ru side of the best C_4S plane.

cymene)Ru]$_3$S$_2^{2+}$.[24] The Ru-S (TMT) distances are ca. 0.04 Å longer at 2.414 (4) to 2.432 (3) Å. X-ray diffraction does not readily distinguish Cl and S atoms, but the location of the sulfur at the triply bridging site is confirmed by the ^{1}H NMR spectroscopy of the cluster.

A striking aspect of the structure is that all three TMT ligands are oriented such that the three thiophenic sulfur atoms are trans with respect to the μ_3-S. Because of this, the cluster has idealized C_{3v} symmetry. With respect to the TMT ligands, the sulfur atoms lay 0.076–0.09 Å above the best C_4S plane, away from the ruthenium atoms. The same effect is seen in $[(TMT)_2Ru]^{2+}$. The methyl groups at positions 3 and 4 on the TMT ring are splayed ~0.2 Å out of the C_4S plane away from the Ru atom.

The formation of the mixed chloro–sulfido cluster was an unexpected result; the corresponding reaction of [(*p*-cymene)RuCl$_2$]$_2$ and $(Me_3Si)_2S$ affords [(*p*-cymene)Ru]$_3$S$_2^{2+}$, a closo trigonal bipyramidal cluster.[24] Isolation of $[(TMT)RuCl]_3S^+$ suggests that [(*p*-cymene)RuCl]$_3$S$^+$ is an intermediate in the assembly of [(*p*-cymene)Ru]$_3$S$_2^{2+}$.

Discussion

Thiophenes are among the most problematic constituents of fossil fuels. They occur widely, and they are less reactive than many other organosulfur compounds in part because of their low basicity.[25] The latter effect has also been a major barrier to the development of thiophene coordination chemistry such that the only thiophene complexes previously available are those with kinetically inert ancillary ligands. This deficiency is addressed by our synthesis of $[(TMT)RuCl_2]_2$.

Thiophenes can be catalytically desulfurized by treatment with hydrogen over various metal sulfide catalysts (eq 4). Molybdenum

$$R_4C_4S \xrightarrow[\text{M catalyst}]{H_2} \text{alkenes, alkanes} + H_2S \qquad (4)$$

catalysts are widely used in industry although more recent work has shown that the Ru-, Os-, Rh-, and Ir-based catalysts are highly active.[26]

Somorjai and co-workers[27] showed that partially sulfided Mo and Re surfaces catalyze thiophene hydrodesulfurization, although less well than clean metals. Studies on a variety of metals[5a,6,27] implicate η^5 bonding as the prevalent chemisorption mode for thiophene at low coverages. This background suggests that $[(TMT)RuCl]_3S^+$ is a good molecular representation of thiophene chemisorbed on a RuS_2-derived[26] catalyst. This cation is multimetallic, comprised of catalytically relevant metals, partially sulfided, and contains π-bonded thiophene.

In view of the extensive chemistry known for compounds of the type $[(arene)RuCl_2]_2$,[28] there is considerable scope for further studies using **1**. The synthetic flexibility offered by **1** has allowed us to determine some of the properties of the $(TMT)Ru^{2+}$ fragment. The lability of $[(TMT)Ru(CH_3CN)_3]^{2+}$ vs the stability of [(*p*-cymene)Ru(CH$_3$CN)$_3$]$^{2+}$ is striking. This may be a kinetic effect in view of the ability of thiophene to adopt an η^1-S-bonding mode.[7-9] Similarly [(*p*-cymene)RuCl]$_2$WS$_4$ and (*p*-cymene)-RuWS$_4$(PPh$_3$) are robust while the TMT analogues cannot be isolated.[29] Still it is unclear why $[(TMT)Ru(CH_3CN)_3]^{2+}$ should be labile while $[(TMT)Ru(H_2O)_3]^{2+}$ is kinetically robust. The contrasting reactivities of $[(TMT)RuCl_2]_2$ and [(*p*-cymeme)-RuCl$_2$]$_2$ toward $(Me_3Si)_2S$ suggests that the Ru–Cl bonds are stronger in TMT complexes than in *p*-cymene analogues.[30] Finally, we have presented structural results that show the decided tendency of the TMT ligand to adapt to the octahedral coordi-

---

[24] Lockemeyer, J. R.; Rauchfuss, T. B.; Rheingold, A. L. *J. Am. Chem. Soc.* **1989**, *111*, 5733.

[25] Thiophene in coal: Attar, A.; Hendrickson, G. S. In Coal Structure; Meyers, R. A., Ed.; Academic Press: New York, 1982. Thiophene in petroleum: Galpern, G. D. In *Thiophene and Its Derivatives*; Gronowitz, S., Ed.; Wiley: New York, 1985.

[26] Chianelli, R. R. *Catal. Rev. Sci. Eng.* **1984**, *26*, 361.

[27] Gellman, A. J.; Russell, M. E.; Somorjai, G. A. *J. Catal.* **1987**, *107*, 103. Gellman, A. J.; Nieman, D.; Somorjai, G. A. *Ibid.* **1987**, *107*, 92.

[28] Reviews of Ru–arene chemistry: Bennett, M. A.; Bruce, M. I.; Matheson, T. W. In *Comprehensive Organometallic Chemistry*; Wilkinson, G., Stone, F. G. A., Abel, E. W., Eds.; Pergamon: Oxford, 1982; Vol. 4, pp 796–803. Moriarity, R. M.; Gill, U. S.; Ku, Y. Y. *J. Organometal. Chem.* **1988**, *350*, 157.

[29] Howard, K. E.; Lockemeyer, J. R.; Ogilvy, A. E.; Rauchfuss, T. B.; Wilson, S. R.; Yang, X. Manuscript in preparation.

[30] $(Me_3Si)_2S$ is widely used to effect S^{2-} for $2Cl^-$ exchange; see: Fenske, D.; Ohmer, J.; Hachgenei, J.; Merzweiler, K. *Angew. Chem., Int. Ed. Engl.* **1988**, *27*, 1277; *Angew. Chem.* **1988**, *100*, 1300.

Table III. NMR Data for (Tetramethylthiophene)ruthenium(II) Complexes[a]

compd	TMT C*H*$_3$ protons	others
TMT[b]	2.28 (s), 1.98 (s)	^{13}C: 132.9, 127.7, 12.9, 12.6
[(TMT)RuCl$_2$]$_2$[c] (**1**)	2.06 (s), 1.97 (s)	^{13}C: 92.1, 89.1, 12.8, 10.8
[(TMT)Ru(D$_2$O)$_3$](BF$_4$)$_2$[d]	1.94 (s), 1.87 (s)	
(TMT)RuCl$_2$(PPh$_3$)	1.99 (br), 1.66 (br)	7.70 (t, 2 H), 7.37 (m, 3 H)
(TMT)RuCl$_2$(PPh$_3$)[e]	2.04 (s, 3 H), 2.02 (s, 3 H), 1.54 (br s, 3 H), 1.02 (s, 3 H)	
(TMT)RuCl$_2$(P(tol)$_3$)	2.00 (br), 1.66 (br)	7.56 (t, 2 H), 7.12 (d, 2 H), 2.34 (s, 9 H, C*H*$_3$)
(TMT)RuCl$_2$(PMe$_3$)	1.99 (s), 1.92 (s)	1.54 (d, 9 H, (C*H*$_3$)$_3$P)
(TMT)Ru(OTf)$_2$(PMe$_3$)[f]	2.03 (s), 2.00 (s)	1.51 (d, 9 H, (C*H*$_3$)$_3$P)
(TMT)RuCl$_2$(PBu$_3$)	1.98 (s), 1.96 (s)	1.97 (t, 6 H, C*H*$_2$P), 1.38 (br m, 12 H, CH$_3$C*H*$_2$C*H*$_2$CH$_2$P), 0.91 (t, 9 H, Me)$^+$
(TMT)RuCl$_2$(*p*-toludine)	1.90 (s), 1.65 (s)	7.28 (q, 2 H, C$_6$*H*$_4$), 7.09 (q, 2 H, C$_6$*H*$_4$), 5.46 (br s, 2 H, N*H*$_2$), 2.30 (s, 3 H C*H*$_3$)
[(TMT)$_2$Ru](BF$_4$)$_2$[g]	2.53 (s), 2.34 (s)	^{13}C: 111.0, 107.7, 13.5, 10.99
[(*p*-cymene)(TMT)Ru](PF$_6$)$_2$[h]	2.58 (s), 2.52 (s)	^{13}C: 113.9, 107.9, 13.7, 12.2
[(TMT)RuCl]$_3$S(PF$_6$)	2.04 (s), 1.89 (s)	

[a] Measured in CDCl$_3$ at 24 °C unless otherwise noted. Chemical shifts (δ) are relative to internal Me$_4$Si. Abbreviations: s = singlet, d = doublet, t = triplet, q = quartet, m = multiple, br = broad. [b] Reference 11. Other solvents: Me$_2$CO (2.21, 1.93); C$_6$D$_6$ (2.09, 1.78); CD$_3$CN (2.23, 1.96); CD$_2$Cl$_2$ (2.26, 1.98). [c] D$_2$O solution: 1.94 (s), 1.87 (s), 1.79 (s). [d] D$_2$O solution. [e] CD$_2$Cl$_2$ solution at −60 °C. [f] Generated in situ from (TMT)RuCl$_2$(PMe$_3$) in CD$_2$Cl$_2$ solution. [g] (CD$_3$)$_2$CO solution. In D$_2$O, the ^{1}H NMR resonances were 2.20 (s), 2.02 (s), 2.01 (s). [h] Reference 11, (CD$_3$)$_2$CO solution.

Table IV. Analytical Data for (Tetramethylthiophene)ruthenium(II) Complexes (Theoretical Values in Parentheses)

complex	C	H	S	Cl
[(TMT)RuCl$_2$]$_2$ (**1**)	30.63 (30.78)	3.81 (3.87)	9.66 (10.27)	23.69 (22.71)
(TMT)RuCl$_2$(PPh$_3$)	53.67 (54.36)	4.70 (4.74)	5.50 (5.58)	12.55 (12.34)
(TMT)RuCl$_2$(PMe$_3$)	34.43 (34.03)	5.55 (5.45)	8.85 (8.26)	19.34 (18.26)
(TMT)RuCl$_2$(PBu$_3$)	46.29 (46.69)	7.59 (7.64)	6.16 (6.23)	13.91 (13.78)
(TMT)RuCl$_2$(*p*-H$_2$NC$_6$H$_4$Me)·CH$_2$Cl$_2$[a]	38.03 (38.11)	4.54 (4.60)	6.46 (6.36)	27.59 (28.12)
(TMT)RuCl$_2$(P(tol)$_3$)	55.96 (56.22)	5.50 (5.37)	5.02 (5.17)	11.97 (11.44)
[(TMT)$_2$Ru](BF$_4$)$_2$[b]	34.56 (34.62)	4.39 (4.36)	11.60 (11.55)	
[(TMT)RuCl]$_3$S(PF$_6$)	28.31 (28.62)	3.59 (3.60)	12.75 (12.73)	9.75 (10.56)

[a] N, 2.78 (2.79). [b] F, 27.31 (27.38).

nation geometry offered by a metal center.

Experimental Section

Ruthenium trichloride was obtained from Johnson Matthey Inc. [(*p*-Cymene)RuCl$_2$]$_2$ was prepared according to Bennett's method,[31] but it is now available from Aldrich. 2,3,4,5-Tetramethylthiophene[32] and (Me$_3$Si)$_2$S[33] (**Caution**: STENCH!) were prepared according to literature methods. Tetrahydrofuran was distilled from Na/K alloy, diethyl ether from sodium benzophenone ketyl, and dichloromethane from P$_4$O$_{10}$. Acetone was stored over activated 4-Å sieves for several days. The instrumentation used in this project is the same as that described in ref 24. NMR and microanalytical results are set out in Tables III and IV.

[(TMT)RuCl$_2$]$_2$. [(*p*-Cymene)RuCl$_2$]$_2$ (5.00 g, 8.16 mmol) and TMT (25 mL) were placed in a 100-mL Schlenk flask with a Teflon-coated magnetic stir bar. The mixture was purged with N$_2$ and then immersed in an oil bath at 210 °C. Soon after the initial heating, the cymene dimer dissolved and deposited a dark red crystalline solid on the walls of the Schlenk flask. The mixture was heated at this temperature for 6 h with periodic flushing of the vapor phase with N$_2$ via a syringe needle to remove liberated cymene. The mixture was then cooled to room temperature, filtered on a glass frit to remove unreacted TMT, and washed with hexanes. The crude product was extracted into ca. 500 mL of CH$_2$Cl$_2$ and filtered to remove an insoluble black solid. The filtrate was concentrated in vacuo to a volume of ca. 25 mL, and 5 mL of hexanes was slowly added to complete the precipitation. The solid product was washed with 2 mL of CH$_2$Cl$_2$ followed by hexanes and dried in vacuo to give 3.34 g (65%) of red microcrystals. Along with the formation of [(TMT)RuCl$_2$]$_2$, a substantial quantity of CH$_2$Cl$_2$-insoluble black solid was formed, which dissolved in ionizing solvents such as CH$_3$CN, DMF, CH$_3$NO$_2$, and H$_2$O to give green solutions. Also found in the reaction mixture was a white organic-soluble mixture. EI-MS data on the white solids suggest coupled thiophene products.

[(TMT)Ru(H$_2$O)$_3$]$^{2+}$. A solution of **1** in D$_2$O shows ^{1}H NMR signals at 1.94, 1.87, and 1.79 ppm with relative intensities of 17:130:118. Treatment of this solution with 2 equiv of AgOTf followed by filtration gave a yellow solution that exhibited equally intense peaks at 1.94 and 1.87.

[(TMT)$_2$Ru](BF$_4$)$_2$. To a mixture of **1** (300 mg, 0.480 mmol) and TMT (0.5 mL) in 30 mL of acetone was added solid AgBF$_4$ (374 mg, 1.922 mmol). The resulting mixture was stirred for 1 h and then filtered through Celite. The orange filtrate was concentrated to a volume of 5 mL and diluted with 5 mL of CH$_2$Cl$_2$. The product was precipitated by slow addition of diethyl ether, filtered, and washed with CH$_2$Cl$_2$ and Et$_2$O. After vacuum drying, we obtained 445 mg (83%) of a yellow microcrystalline solid. The corresponding triflate salt was prepared in 86% yield using AgOTf in place of AgBF$_4$.

Reaction of [(TMT)RuCl$_2$]$_2$ with PPh$_3$ in Hexanes. A suspension of **1** (72 mg, 0.115 mmol) and PPh$_3$ (131 mg, 0.500 mmol) in 25 mL of hexanes was refluxed with stirring for 4 h, during which time a salmon-colored powdered formed. The solid was filtered, washed with hexanes, and air dried. The crude product was recrystallized from CH$_2$Cl$_2$/hexanes and dried in vacuo to give 80 mg of brown–red microcrystals which had the following analysis: C, 41.87; H, 4.42; Cl, 19.09; S, 8.23.

(TMT)RuCl$_2$(PR$_3$). The procedure for the preparation of (TMT)RuCl$_2$((*p*-tolyl)$_3$P) is typical. To a mixture of [(TMT)RuCl$_2$]$_2$ (200 mg, 0.320 mmol) in 20 mL of CH$_2$Cl$_2$ was added a solution of tri-*p*-tolylphosphine (195 mg, 0.640 mmol) in 15 mL of CH$_2$Cl$_2$. The resulting red solution was stirred for 45 min, concentrated to 10 mL, and diluted with 10 mL of hexanes. The product was filtered in air, washed with hexanes, and dried in vacuo to give 385 mg (97%) of a red–pink microcrystalline solid. Yields for the related complexes are as follows: P(C$_6$H$_5$)$_3$, 86%; PMe$_3$, 91%; P(*n*-Bu)$_3$, 91%.

(TMT)RuCl$_2$(*p*-CH$_3$C$_6$H$_4$NH$_2$). A solution of *p*-toluidine (69 mg, 0.641 mmol) in CH$_2$Cl$_2$ (10 mL) was added to a suspension of **1** (200 mg, 0.310 mmol) in CH$_2$Cl$_2$ (10 mL). The resulting bright red solution soon afforded a red-orange precipitate. The suspension was stirred for 1 h, then 10 mL hexanes was added to complete precipitation of the product. The solid was filtered, washed with hexanes, and dried *in vacuo* to give 290 mg (90%) of orange powder.

[(TMT)RuCl]$_3$S(PF$_6$). To a solution of **1** (300 mg, 0.480 mmol) in 150 mL of CH$_2$Cl$_2$ was added (Me$_3$Si)$_2$S (70 μL, 0.33 mmol). The resulting dark red solution was stirred at ambient temperature for 6 h. The solvent was then removed and the solid dried in vacuo for several hours. Water (60 mL) was then added to the crude product, and the

---

(31) Bennett, M. A.; Huang, T.-N.; Matheson, T. W.; Smith, A. K. *Inorg. Synth.* **1981**, *21*, 74.

(32) Gaertner, R.; Tonkyn, R. G. *J. Am. Chem. Soc.* **1951**, *73*, 5872.

(33) Armitage, D. A.; Clark, M. J.; Sinden, A. W.; Wingfield, J. N.; Abel, E. W.; Louis, E. *Inorg. Synth.* **1974**, *15*, 207.

Table V. Atomic Coordinates and Isotropic Thermal Parameters (Å^2) for $[(TMT)_2Ru](BF_4)_2 \cdot 2CH_3NO_2$

	x	*y*	*z*	U^a
Ru	0.2498 (1)	0.7453 (1)	0.5665 (1)	0.027 (1)
S1	0.1595 (2)	0.9065 (2)	0.5011 (1)	0.042 (1)
S2	0.1687 (2)	0.5726 (2)	0.5760 (1)	0.045 (1)
N1	0.2642 (6)	0.2589 (8)	0.3647 (6)	0.069 (4)
N2	0.1046 (6)	0.2567 (7)	0.800 (5)	0.060 (3)
O1	0.2773 (7)	0.3582 (8)	0.3562 (7)	0.112 (5)
O2	0.3123 (7)	0.1855 (10)	0.3473 (6)	0.110 (5)
O3	0.0959 (7)	0.3553 (7)	0.0585 (5)	0.093 (4)
O4	0.0721 (7)	0.1759 (7)	0.0352 (5)	0.096 (4)
C17	0.1848 (9)	0.2251 (10)	0.3975 (8)	0.076 (5)
C18	0.1582 (12)	0.2318 (12)	0.1636 (7)	0.094 (6)
B1	0.0623 (4)	0.6031 (3)	0.7653 (3)	0.070 (6)
B2	0.3969 (1)	0.2527 (1)	0.0930 (1)	0.092 (7)
F1	0.0672 (6)	0.5910 (7)	0.6963 (3)	0.223 (9)
F2	0.0948 (1)	0.5134 (1)	0.8053 (1)	0.256 (11)
F3	−0.0285 (4)	0.6201 (7)	0.7610 (5)	0.180 (7)
F4	0.1155 (7)	0.6880 (2)	0.7985 (6)	0.255 (11)
F5	0.3371 (3)	0.3308 (5)	0.0990 (2)	0.161 (7)
F6	0.3511 (4)	0.1575 (2)	0.0808 (3)	0.237 (9)
F7	0.4279 (2)	0.2753 (7)	0.0357 (1)	0.263 (12)
F8	0.4712 (1)	0.2474 (1)	0.1563 (1)	0.214 (14)
C1	0.1750 (7)	0.8927 (7)	0.6026 (5)	0.043 (3)
C2	0.2760 (6)	0.8978 (7)	0.6484 (5)	0.043 (3)
C3	0.3411 (7)	0.9025 (7)	0.6018 (6)	0.050 (3)
C4	0.2918 (6)	0.9049 (7)	0.5206 (5)	0.039 (3)
C5	0.0846 (7)	0.8891 (9)	0.6292 (6)	0.064 (4)
C6	0.3110 (9)	0.8969 (10)	0.7367 (6)	0.076 (5)
C7	0.4552 (7)	0.9112 (10)	0.6352 (7)	0.072 (5)
C8	0.3338 (8)	0.9200 (10)	0.4537 (7)	0.073 (5)
C9	0.2933 (6)	0.5921 (7)	0.6399 (5)	0.041 (3)
C10	0.3603 (6)	0.6025 (7)	0.5974 (5)	0.040 (3)
C11	0.3158 (6)	0.6020 (7)	0.5156 (5)	0.046 (3)
C12	0.2058 (7)	0.5886 (8)	0.4912 (5)	0.046 (3)
C13	0.3145 (8)	0.5795 (10)	0.7273 (6)	0.070 (5)
C14	0.4761 (7)	0.6083 (10)	0.6400 (7)	0.068 (5)
C15	0.3661 (8)	0.6088 (11)	0.4549 (7)	0.075 (5)
C16	0.1339 (7)	0.5766 (10)	0.4120 (5)	0.060 (4)

[a] Equivalent isotropic *U* defined as one-third of the trace of the orthogonalized U_{ij} tensor.

Table VI. Crystallographic Data for $[(TMT)_2Ru](BF_4)_2 \cdot 2CH_3NO_2$

formula	$C_{16}H_{24}RuS_2F_8 \cdot 2CH_3NO_2$
crystal system	monoclinic
space group	$P2_1/c$
a, Å	14.061 (3)
b, Å	11.685 (3)
c, Å	17.923 (4)
β, deg	109.10 (2)
V, Å^3	2782.7 (11)
Z	4
D(calcd), g cm^{-3}	1.463
μ(Mo Kα), cm^{-1}	7.74
color	yellow
size, mm	0.30 × 0.31 × 0.34
temp, K	295
T_{max}/T_{min}	1.12
diffractometer	Nicolet R3m
radiation	Mo Kα
wavelength, Å	$\lambda = 0.71073$
scan limits, deg	$4 \le 2\theta \le 55$
scan method	Wyckoff
rflns collected	6915
indpdt rflns	6389
R(int), %	4.0
obs rflns ($3\sigma F_o$)	4142
std rflns	3 std/197 rflns
var in stds, %	<1
R(*F*), %	6.53
R(*wF*), %	7.05
GOF	1.465
Δ/σ (final)	0.042
$\Delta\rho$, e Å^{-3}	1.25

Table VII. Crystallographic Data for $[(TMT)RuCl]_3S[PF_6]$

formula	$[Ru_3Cl_3S(SC_8H_{12})_3][PF_6]$
crystal system	orthorhombic
space group	*Pbca*
a, Å	32.480 (2)
b, Å	15.349 (1)
c, Å	13.673 (1)
V, Å^3	6816 (1)
Z	8
density (calc), g/cm^3	1.963
color, habit	red, plate
dimensions {form} or (face), mm	{1 0 0}, 0.07; (−1 1 3), 0.23; (0 1 −3), 0.23; (0 − 1 0), 0.24; (−1 2 1), 0.24
diffractometer	Syntex $P2_1$
μ, cm^{-1}	18.58
transmission factor range	0.775–0.454 (numerical)
2θ limit, deg (octants)	3.0–49.0 ($+h+k+l$) 3.0–7.0 ($\pm h \pm k \pm l$)
intensities (unique, R_i)	6636 (6424, 0.013)
intensities > $2.58\sigma(I)$	3297
R	0.047
R_w (for $w = 1/\sigma^2(F_o) + pF_o^2$)	0.062 ($p = 0.02$)
max density in ΔF map, e/Å^3	0.82

Table VIII. Atomic Coordinates and Isotropic Thermal Parameters for $[(TMT)RuCl]_3S[PF_6]$

	x/*a*	*y*/*b*	*z*/*c*	$U_{eq}{}^a$
Ru1	0.09580 (3)	0.47768 (6)	0.18499 (6)	0.0373 (5)
Ru2	0.13652 (3)	0.31086 (6)	0.34294 (6)	0.0344 (5)
Ru3	0.19720 (3)	0.49883 (6)	0.28117 (6)	0.0345 (5)
Cl1	0.10648 (9)	0.3203 (2)	0.1794 (2)	0.045 (2)
Cl2	0.20367 (8)	0.3392 (2)	0.2666 (2)	0.045 (2)
Cl3	0.16532 (9)	0.4952 (2)	0.1190 (2)	0.048 (2)
S1	0.13026 (8)	0.4643 (2)	0.3385 (2)	0.035 (2)
S2	0.0508 (1)	0.5107 (2)	0.0495 (3)	0.062 (2)
S3	0.1362 (1)	0.1576 (2)	0.3877 (2)	0.055 (3)
S4	0.2645 (1)	0.5626 (2)	0.2500 (2)	0.051 (2)
C1	0.0322 (4)	0.4629 (9)	0.1589 (10)	0.063 (8)
C2	0.0362 (3)	0.5164 (8)	0.2406 (10)	0.050 (6)
C3	0.0609 (4)	0.5938 (8)	0.2192 (10)	0.060 (9)
C4	0.0747 (4)	0.5956 (8)	0.1213 (9)	0.051 (8)
C5	0.0083 (3)	0.3759 (9)	0.1526 (11)	0.069 (7)
C6	0.0171 (5)	0.5027 (9)	0.3378 (10)	0.073 (10)
C7	0.0688 (5)	0.6627 (9)	0.2915 (12)	0.087 (10)
C8	0.0976 (4)	0.6652 (8)	0.0650 (11)	0.079 (10)
C9	0.1625 (4)	0.2356 (7)	0.4582 (8)	0.045 (8)
C10	0.1359 (4)	0.2966 (7)	0.5002 (7)	0.038 (8)
C11	0.0942 (4)	0.2881 (8)	0.4655 (8)	0.046 (8)
C12	0.0917 (4)	0.2227 (8)	0.3936 (8)	0.051 (8)
C13	0.2072 (4)	0.2179 (9)	0.4829 (9)	0.066 (9)
C14	0.1489 (4)	0.3603 (8)	0.5777 (8)	0.062 (10)
C15	0.0592 (4)	0.3446 (9)	0.5028 (10)	0.072 (10)
C16	0.0524 (5)	0.1905 (10)	0.3454 (10)	0.079 (10)
C17	0.2524 (3)	0.5095 (9)	0.3616 (8)	0.047 (6)
C18	0.2221 (4)	0.5551 (8)	0.4131 (8)	0.047 (8)
C19	0.2039 (3)	0.6198 (7)	0.3592 (8)	0.042 (7)
C20	0.2193 (3)	0.6284 (8)	0.2633 (8)	0.045 (6)
C21	0.2807 (4)	0.4375 (9)	0.3947 (10)	0.061 (9)
C22	0.2135 (4)	0.5379 (9)	0.5218 (8)	0.062 (10)
C23	0.1706 (4)	0.6806 (9)	0.4010 (10)	0.074 (10)
C24	0.2100 (4)	0.6932 (8)	0.1843 (9)	0.062 (9)
P	0.3928 (1)	0.4201 (2)	0.2180 (3)	0.063 (2)
F1	0.3536 (3)	0.4801 (6)	0.2302 (7)	0.099 (6)
F2	0.3912 (6)	0.3920 (14)	0.3202 (10)	0.24 (2)
F3	0.3657 (3)	0.3430 (8)	0.1922 (15)	0.203 (9)
F4	0.4324 (3)	0.3607 (6)	0.1998 (8)	0.111 (6)
F5	0.3930 (5)	0.4423 (10)	0.1062 (9)	0.17 (1)
F6	0.4202 (4)	0.4955 (7)	0.2357 (16)	0.203 (8)

[a] U_{eq} is calculated as one-third the trace of the anisotropic tensor.

mixture was stirred for 10 min. The resulting red–orange solution was filtered through Celite, washing with additional H_2O. Solid KPF_6 (500 mg) was added to the red–orange filtrate. The resulting precipitate was filtered, washed with a small quantity of water, and air dried. The solid was then extracted into CH_2Cl_2 and filtered. The Na_2SO_4-dried red–orange solution was then concentrated in vacuo to 15 mL and slowly diluted with 5 mL of hexanes. Further concentration gave a rust-colored powder that was filtered, washed with hexanes and Et_2O, and dried in vacuo. Yield 234 mg (73%). FAB MS: M^+ calcd (found) 863 (863.5).

X-ray Crystallography. **$[(TMT)_2Ru](BF_4)_2\cdot 2CH_3NO_2$.** Crystals suitable for the X-ray diffraction study were grown by vapor diffusion of benzene into a nitromethane solution of the complex. A nearly equidimensional cube was cut from a larger crystal. Axial photographs and systematic absences in the data uniquely identified the space group. Corrections for absorption were unnecessary. The structure was solved by a Patterson synthesis and developed from difference maps. The lattice was found to contain two molecules of nitromethane for each [cation]-[anion]$_2$ formula. Both the solvent molecules and the anions were thermally active, leading to a somewhat elevated final *R* factor. All non-hydrogen atoms were refined with anisotropic thermal parameters, and all hydrogen atoms were idealized (d(CH) = 0.96 Å). The BF_4^- atoms were constrained to rigid tetrahedra; a common B–F distance was refined to 1.268 (3) Å, a value somewhat smaller than the usual value of ~1.36 Å. All computations used SHELXTL (5.1) software (Nicolet XRD, Madison, WI). Crystal, data collection, and refinement parameters are listed in Table V. Atomic coordinates and isotropic thermal parameters are listed in Table VI.

$[(TMT)RuCl]_3S(PF_6)$. Crystals suitable for X-ray diffraction were grown by vapor diffusion of diethyl ether into a nitromethane solution of the cluster. A red, translucent platy crystal of dimensions 0.1 × 0.5 × 0.5 mm was cut from a larger crystal. Axial photographs and systematic absences unambiguously defined the space group. Corrections for absorption were applied, with maximum and minimum transmission factors of 0.775 and 0.454, respectively. The structure was solved by direct methods (SHELX-86). The correct Ru atom positions were deduced from an *E* map. Subsequent least-squares-difference Fourier calculations (SHELX-76) revealed positions for the remaining non-hydrogen atoms. All non-hydrogen atoms were refined with anisotropic thermal parameters, and all hydrogen atoms were idealized. The anisotropic thermal parameters for the fluorine atoms converged to inordinately high values. There was no clear indication of disorder for these positions so the high thermal parameters were retained; consequently, some of the P–F bond lengths converged significantly shorter than expected. Crystal, data collection, and refinement parameters are listed in Table VII. Atomic coordinates and isotropic thermal parameters are listed in Tables VIII.

Acknowledgment. This research was supported by the National Science Foundation. We acknowledge the support of the Petroleum Research Fund, administered by the American Chemical Society. Ruthenium trichloride was obtained on loan from Johnson Matthey. We thank Anton E. Skaugset and Ann E. Ogilvy for gifts of the tetramethylthiophene and for useful discussions.

Supplementary Material Available: Tables of calculated and observed structure factors (28 pages). Ordering information is given on any current masthead page.

Silicon-Directed Decarbonylation of Trimethylsilyl β,γ-Enals by Photolysis

Jih Ru Hwu*,† and Paul S. Furth

Contribution from the Department of Chemistry, The Johns Hopkins University, Baltimore, Maryland 21218. Received July 8, 1988

Abstract: Irradiation of cis trimethylsilyl aldehyde **9** with UV light generated by a medium-pressure mercury lamp with Pyrex glass filter gave decarbonylated product **11** in 98% yield. Under the same conditions, the corresponding trans trimethylsilyl aldehyde **10** was decarbonylated to afford the same product (**11**) in 89% yield. The trimethylsilyl group directed the fragmentation of the diyls generated from **9** and **10** by preventing oxa-di-π-methane rearrangement and the 1,3 formyl migration. The results indicated that the alkyl radical intermediates, generated by photolysis, can be stabilized by a trimethylsilyl group at the β position; these β-trimethylsilyl alkyl radicals did not eliminate to give alkenes and trimethylsilyl radicals. By use of the stabilizing effect exerted by silicon, photolysis of cis trimethylsilyl aldehyde **33** gave a 98% yield of isomeric trimethylsilyl alkenes **34–36** in a ratio of 10.9:1.0:1.4. Similarly, photolysis of the corresponding trans trimethylsilyl aldehyde **37** afforded a 83% yield of the same products in a ratio of 1.0:25.5:1.6. Furthermore, cis trimethylsilyl aldehyde **38** was photolyzed to produce a 98% yield of isomeric trimethylsilyl alkenes **39–41** in a ratio of 10.9:1.3:1.0; trans trimethylsilyl aldehyde **42** gave a 99% yield of the same trimethylsilyl alkenes in a ratio of 0.1:32.0:1.0. In all of these decarbonylations, the trimethylsilyl group remained in the reaction products.

A Me_3Si group at the β position can stabilize an alkyl radical by ~2.6–2.8 kcal/mol;[1,2] the β-trimethylsilyl alkyl radical normally does not eliminate to give an alkene and $Me_3Si^\bullet$ (Scheme I).[3-5] A Me_3Si group at the β position can stabilize a carbocation by ~38 kcal/mol;[6,7] nevertheless the β-trimethylsilyl carbocation fragments to give an alkene and Me_3Si^+.[8] Although the stabilizing effect of the Me_3Si group has been widely utilized to control reactions with carbocationic intermediates,[8a,9] very few applications involving radicals have been reported.[10] We intended to use the stabilizing ability of the Me_3Si group to direct decarbonylations, which involved radical intermediates.

The decarbonylation of aldehydes occurs in biological systems, such as in the degradation of fatty acids to alkanes via the intermediate octadecanal.[11] Oxidative decarbonylations may be responsible for the conversion of lanosterol to 14-desmethyllanosterol[12] and the transformation of androgens to estrogens.[13]

Scheme I

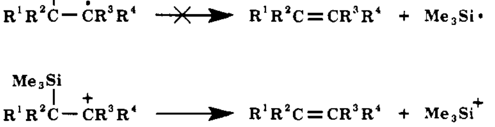

$$\mathrm{R^1R^2\overset{Me_3Si}{\overset{|}{C}}-\dot{C}R^3R^4} \not\longrightarrow \mathrm{R^1R^2C{=}CR^3R^4 + Me_3Si\cdot}$$

$$\mathrm{R^1R^2\overset{Me_3Si}{\overset{|}{C}}-\overset{+}{C}R^3R^4} \longrightarrow \mathrm{R^1R^2C{=}CR^3R^4 + Me_3Si^+}$$

The decarbonylation of aldehydes by other chemical means is generally accomplished by use of light,[14] high temperatures,

---

[†] Research fellow of the Alfred P. Sloan Foundation (1986–1990).

(1) Auner, N.; Walsh, R.; Westrup, J. *J. Chem. Soc., Chem. Commun.* **1986**, 207.

(2) Davidson, I. M. T.; Barton, T. J.; Hughes, K. J.; Ijadi-Maghsoodi, S.; Revis, A.; Paul, G. C. *Organometallics* **1987**, *6*, 644.

(3) Bennett, S. W.; Eaborn, C.; Jackson, R. A.; Pearce, R. *J. Organomet. Chem.* **1968**, *15*, P17.

(4) Jackson, R. A. *J. Chem. Soc., Chem. Commun.* **1974**, 573.

0002-7863/89/1511-8834$01.50/0